

ELF DOSAGE IN ELLIPSOIDAL MODELS OF MAN DUE TO HIGH  
VOLTAGE TRANSMISSION LINES

Francis X. Hart, Ph.D.

Department of Physics, University of the South, Sewanee, TN 37375

Andrew A. Marino, Ph.D.

LSU Medical Center, P. O. Box 33932, Shreveport, LA 71130

ABSTRACT

The fields, flux, and power density produced inside an ellipsoidal model of man by overhead high-voltage transmission lines have been calculated. The values depend strongly on the conductivity and the shape of the ellipsoid and, in general, vary from point to point within it. The maximum energy flux is the more reliable indicator of exposure to the electromagnetic field.

INTRODUCTION

There are numerous reports of non-thermal biological effects due to microwave radiation at incident flux levels of 1-1000  $\mu\text{W}/\text{cm}^2$  (1-10). These include changes in the endocrine, cardiovascular, and nervous systems, as well as alterations in behavior. Similar effects have been reported following exposure to radio-frequency and extremely-low-frequency (ELF) fields (10-22). The production of similar kinds of biological responses at such diverse frequencies suggests the existence of basic frequency-independent processes by which electromagnetic energy can affect living organisms. But since electromagnetic energy at different frequencies interacts differently with biological systems, it is difficult to determine the most

important electrical parameters with regard to the production of similar kinds of biological effects at different frequencies. One can not, for instance, compare incident energy fluxes because parameters such as penetration depth and reflection coefficient differ greatly between opposite ends of the nonionizing electromagnetic spectrum. Consequently those biological effects of nonionizing radiation which occur at different frequencies, such as biological stress (10), cannot be analyzed solely in terms of exposure parameters because the levels of the various electrical parameters inside the biological system (dose) are inherently frequency dependent.

Two quite different external energy fluxes are presently associated with the threshold for biological effects of nonionizing radiation at microwave frequencies, namely  $10 \mu\text{W}/\text{cm}^2$  in the Soviet Union and Eastern Europe, and  $10,000 \mu\text{W}/\text{cm}^2$  in the United States. Although, technically, both values are exposure levels, they may be regarded as doses because up to 100% of the energy is absorbed by the biological system. Employing appropriate mathematical techniques, one can find the flux at other frequency bands that produces the same dose to biological systems as that provided by any specified microwave flux. Such calculations could provide an objective basis upon which to extrapolate microwave exposure levels, at least until definitive biological experiments can be performed. Moreover, the calculations are of interest because of the light they shed on the nature of the interaction between electromagnetic fields and biological systems. In this paper we present such a calculation for the ELF portion of the spectrum.

For reasons of relevance and convenience we shall assume that the source of the ELF flux is a high voltage transmission line. We previously described the exposure fluxes that are associated with a typical 765 kv transmission line (23). It remains therefore to determine the dose that such a line delivers to an appropriate mathematical model of a biological system.

Analytical models for biological systems exposed to ELF fields include spheres (24), prolate spheroids (25), concentric cylinders (26), and two-layer rectangular solids (27). Each such model is useful, but none is clearly superior as a tool for the study of electromagnetic interactions. We have employed an ellipsoidal model of a human being because of the generality and relative morphological realism afforded by an ellipsoid, and because it permits a solution in closed form.

## THEORY

### Direct Electric Field

For ELF fields, the dimensions of biological objects are small in comparison to the wavelength of the radiation and the quasi-static approximation may be used. Figure 1 illustrates an ellipsoid with axes  $a > b > c$ , dielectric constant  $K_1$  and conductivity  $g_1$  embedded in a medium with dielectric constant  $K_2$  and conductivity  $g_2$ . A uniform alternating field of angular frequency is applied in the +X direction by electrodes in the Y-Z plane whose separation is much greater than the dimensions of the ellipsoid. Since there is no free charge in either the internal or external medium, Laplace's equation holds everywhere.

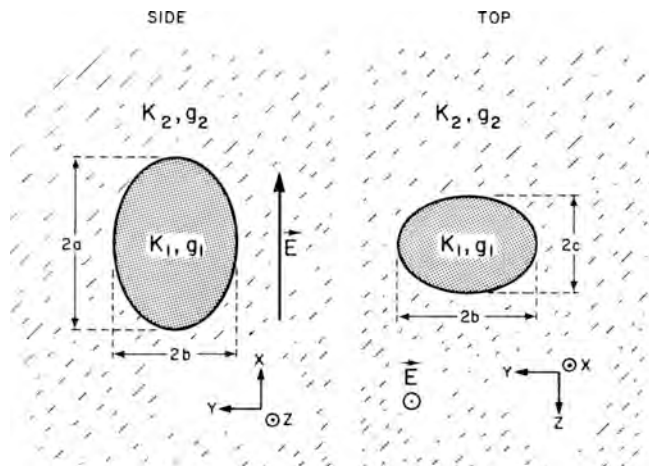


FIGURE 1

Ellipsoid in a Medium of Differing Dielectric Constant and Conductivity.

The solution is similar to that obtained for a dielectric ellipsoid in a uniform, static field (28). Let  $u$ ,  $v$ , and  $p$  be the ellipsoidal coordinates of a point. A family of ellipsoids is parameterized by  $u$ , with the surface of the given ellipsoid corresponding to  $u = 0$ . Outside the ellipsoid  $u > 0$ , inside,  $u < 0$ . The coordinates  $v$  and  $p$  parameterize hyperboloids on surfaces of constant  $u$ .

If  $V_1$  and  $V_2$  represent the potential inside and outside the ellipsoid respectively, then far from the ellipsoid  $V_2$  is given in rectangular coordinates by

$$V_2 \rightarrow -(E_{2A} \cos \omega t + E_{2B} \sin \omega t)x, \quad (1)$$

where  $E_{2A}$  and  $E_{2B}$  are the electric fields associated with the cosine and sine phases of the electric field respectively. Such a distinction becomes useful if an ellipsoid is placed in a uniform field whose phases are specified separately. In ellipsoidal coordinates the usual expression for the potential outside the

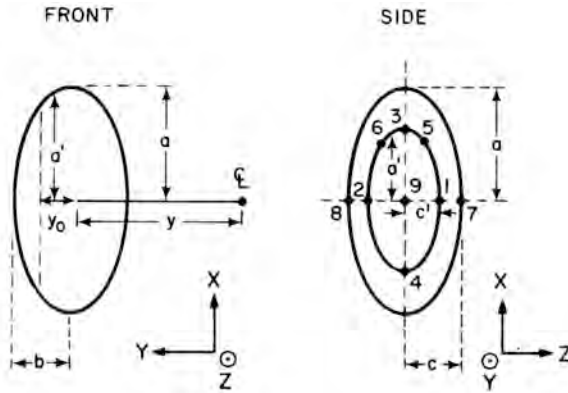


FIGURE 2  
Ellipsoid Located Laterally from the Center-Line of a Transmission Line.

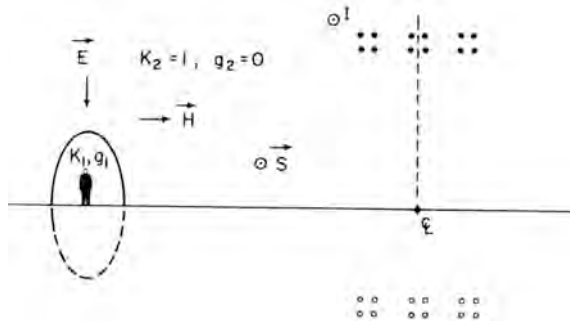


FIGURE 3  
Ellipsoid Model of a Human Being near a Three-Phase 765 KV Transmission Line.

ellipsoid in a static field (28) may be extended to the alternating case as

$$V_2 = F_1(u)F_2(v)F_3(p)\left((C_{1A} + C_{2A}I(u))\cos \omega t + (C_{1B} + C_{2B}I(u))\sin \omega t\right),$$

where

$$F_1(u) = (u + a^2)^{1/2}, F_2(v) = (v + a^2)^{1/2}, F_3(p) = (p + a^2)^{1/2}$$

$$I(u) = \int_u^{\infty} \frac{du}{(u+a^2)((u+a^2)(u+b^2)(u+c^2))^{1/2}}, \quad (3)$$

and the  $C_s$  are constants to be determined by the boundary conditions.

Since  $I(u) \rightarrow 0$  for large  $u$ , far from the ellipsoid

$$V_2 \rightarrow \left( (u+a^2)(v+a^2)(p+a^2) \right)^{1/2} (C_{1A} \cos \omega t + C_{1B} \sin \omega t).$$

Use of the transformation from ellipsoidal to rectangular coordinates (29),

$$x = \left( (u+a^2)(v+a^2)(p+a^2) / (b^2-a^2)(c^2-a^2) \right)^{1/2}, \quad (4)$$

yields

$$V_2 \rightarrow (C_{1A} \cos \omega t + C_{1B} \sin \omega t) x \left( (b^2-a^2)(c^2-a^2) \right)^{1/2}. \quad (5)$$

Comparison of equations (1) and (5) leads to

$$C_{1A} = -E_{2A} / D \quad (6)$$

$$C_{1B} = -E_{2B} / D \quad (7)$$

where

$$D = \left( (b^2-a^2)(c^2-a^2) \right)^{1/2},$$

Inside the ellipsoid (29)

$$V_1 = F_1(u)F_2(v)F_3(p)(C_{3A} \cos \omega t + C_{3B} \sin \omega t) \quad (8)$$

where  $C_{3A}$  and  $C_{3B}$  are to be determined by the boundary conditions which are: (1) continuity of the potential across the interface, i.e.,  $V_1 = V_2$  at  $u = 0$ , and, (2) continuity of the normal ( $n$ ) component of the total current, i.e.,

$$g_2 E_{2n} + K_2 \epsilon_0 \partial E_{2n} / \partial t = g_1 E_{1n} + K_1 \epsilon_0 \partial E_{1n} / \partial t$$

at  $u = 0$ , where  $E_0$  is the permittivity of free space, and

$$E_n = -2 \left( (u + a^2)(u + b^2)(u + c^2) / (u - v)(u - p) \right)^{1/2} \partial V / \partial u.$$

By separately equating the coefficients of the  $\cos \omega t$  and  $\sin \omega t$  terms, one obtains from the first equation

$$C_{1A} + C_{2A} I(0) = C_{3A} \tag{9}$$

$$C_{1B} + C_{2B} I(0) = C_{3B}, \tag{10}$$

and from the second

$$g_2 (C_{1A} + I(0)RC_{2A}) + \omega K_2 \epsilon_0 (C_{1B} + I(0)RC_{2B}) = g_1 C_{3A} + \omega K_1 \epsilon_0 C_{3B} \tag{11}$$

$$g_2 (C_{1B} + I(0)RC_{2B}) + \omega K_2 \epsilon_0 (C_{1A} + I(0)RC_{2A}) = g_1 C_{3B} + \omega K_1 \epsilon_0 C_{3A}, \tag{12}$$

where

$$R = 1 - 2/abcI(0).$$

Simultaneous solution of equations (9)-(12) and application of equations (6) and (7) yield

$$C_{3A} = -(M_1 E_{2A} - M_2 E_{2B}) / D \tag{13}$$

$$C_{3B} = -(M_2 E_{2A} - M_1 E_{2B}) / D \tag{14}$$

$$C_{2A} = -((M_1 - 1)E_{2A} - M_2 E_{2B}) / DI(0) \tag{15}$$

$$C_{2B} = -(M_2 E_{2A} + (M_1 - 1)E_{2B}) / DI(0) \tag{16}$$

where

$$M_1 = Q \left( g_2 (g_1 - Rg_2) + \omega^2 \epsilon_0^2 K_2 (K_1 - RK_2) \right)$$

$$M_2 = Q\omega\epsilon_0(g_2(K_1 - RK_2) - K_2(g_1 - Rg_2))$$

and

$$Q = (1 - R) / \left( \omega^2 \epsilon_0^2 (K_1 - RK_2)^2 + (g_1 - Rg_2)^2 \right).$$

The potentials inside and outside the ellipsoid are obtained by substituting equations (13) and (14) into equation (8), and equations (15) and (16) into equation (2) respectively, with the subsequent utilization of equation (4). This leads to:

$$V_1 = -((M_1 E_{2A} - M_2 E_{2B}) \cos \omega t + (M_2 E_{2A} + M_1 E_{2B}) \sin \omega t) x \quad (17)$$

$$V_2 = \left( (E_{2A} + ((M_1 - 1)E_{2A} - M_2 E_{2B}) I(u)/I(0)) \cos \omega t + (E_{2B} + (M_2 E_{2A} + (M_1 - 1)E_{2B}) I(u)/I(0)) \sin \omega t \right) x \quad (18)$$

The direct field inside the ellipsoid is given by  $\bar{E}_d = -\nabla V_1$ . Using rectangular coordinates one obtains

$$\bar{E}_d = ((M_1 E_{2A} - M_2 E_{2B}) \cos \omega t + (M_2 E_{2A} + M_1 E_{2B}) \sin \omega t) \hat{i}, \quad (19)$$

where  $\hat{i}$  is a unit vector along the X axis, i.e., parallel to the applied field.

As is the case for static fields (28), similar expressions may be obtained for fields with components in the Y and Z directions with the replacement of I(0) by

$$\int_0^\infty \frac{ds}{(s+b^2)((s+a^2)(s+b^2)(s+c^2))^{1/2}}$$

and

$$\int_0^\infty \frac{ds}{(s+c^2)((s+a^2)(s+b^2)(s+c^2))^{1/2}}$$

respectively. The field inside an ellipsoid with an arbitrary orientation relative to an external field may thus be found by decomposing the external field into components in the X, Y, and Z

directions to which the above analysis may separately be applied. Here, for simplicity, we shall assume that the long axis of the ellipsoid is aligned parallel to the applied field (X axis).

### Induced Electric Fields

Near a transmission line, an additional contribution to the internal field is induced by the varying magnetic field. Figure 2 presents two views of a cross sectional slice of an ellipsoid near a transmission line. The X axis is directed vertically; the Y axis is horizontal, perpendicular to the direction of current flow in the line.

It is assumed that the earth behaves as a perfect conductor for both the electric and magnetic fields. At the earth's surface the transmission-line fields are then directed along the X and Y axes respectively and the energy flux along the Z axis. Such an assumption is frequently made (29,30), but it is not as realistic for magnetic as for electric fields. If the earth were not regarded as a perfect conductor, the magnetic field within the ellipsoid would have an additional X component and the induced electric field an additional Y component, and their relative importance would vary with both the distance from the array and the choice of elliptical cross sections. The assumption is used here because the correction for finite conductivity is mathematically complex (31), and would obscure the basic principles under discussion. The error attributable to the perfect-conductor model will be mentioned later.

Consider a slice in the X-Z plane at a distance  $y_0$  from the center of the ellipsoid. Such a cross section is an ellipse with axes  $a' < a$  and  $c' < c$ . At low frequencies the induced electric field  $\bar{E}_i$  is determined by  $\nabla \times \bar{E}_i = -\mu \partial \bar{H} / \partial t$  and  $\nabla \cdot \bar{E}_i = 0$  (32), where

$$\bar{H} = (H_A \cos \omega t + H_B \sin \omega t) \hat{j} \quad (20)$$

is the applied magnetic field and  $\hat{j}$  is a unit vector in the Y direction. It is readily shown that the boundary conditions require that the field lines be ellipses. The induced electric field is found to be

$$\bar{E}_i = \omega \mu_0 (a'^2 + c'^2)^{-1} (a'^2 z \hat{i} - c'^2 x \hat{k}) (H_A \sin \omega t - H_B \cos \omega t) \quad (21)$$

where  $\hat{k}$  is a unit vector in the Z direction and  $\mu_0$  is the permeability of space.

The components of the induced field are then

$$E_x = M_3 (H_A \sin \omega t - H_B \cos \omega t) \quad (22)$$

and

$$E_z = M_4 (H_A \sin \omega t - H_B \cos \omega t) \quad (23)$$

where

$$M_3 = \omega \mu_0 a'^2 z / (a'^2 + c'^2)$$

and

$$M_4 = -\omega \mu_0 c'^2 x / (a'^2 + c'^2)$$

With the axes chosen so that  $a' > c'$  the induced field is a maximum at  $x = 0$  and a minimum at  $z = 0$ .

The total electric field inside an ellipsoid near the line,  $\bar{E}_t$ , is the sum of the direct field  $\bar{E}_d$ , given by equation (19), and the induced field  $\bar{E}_i$ , whose components are given by equations (22) and (23). We thus obtain:

$$\bar{E}_t = \left( (M_1 E_{2A} - M_2 E_{2B} - M_3 H_B) \cos \omega t + (M_2 E_{2A} + M_1 E_{2B} + M_3 H_A) \sin \omega t \right) \hat{i} + (M_4 H_A \sin \omega t - M_4 H_B \cos \omega t) \hat{k} \quad (24)$$

The magnitude of the total field is:

$$E_t = \left( \left( (M_1 E_{2A} - M_2 E_{2B} - M_3 H_B)^2 + M_4^2 H_B^2 \right) \cos^2 \omega t + \left( (M_2 E_{2A} + M_1 E_{2B} + M_3 H_A)^2 + M_4^2 H_A^2 \right) \sin^2 \omega t + 2 \left( (M_1 E_{2A} - M_2 E_{2B} - M_3 H_B) (M_2 E_{2A} + M_1 E_{2B} + M_3 H_A) - M_4^2 H_A H_B \right) \sin \omega t \cos \omega t \right)^{1/2}. \quad (25)$$

### Energy Flux and Power Dissipated

The conduction current density and instantaneous power dissipated per unit volume inside the ellipsoid are respectively

$$\bar{J}_1 = g_1 \bar{E}_t, \quad (26)$$

$$P_1 = g_1 E_t^2. \quad (27)$$

The electrical energy per unit volume stored in the field is

$$W = \varepsilon_0 K_1 E_t^2 / 2 \quad (28)$$

The time averaged electrical power dissipated per unit volume per cycle is  $\bar{P} = \int_0^T P_1 dt / T$ , where  $T = 2\pi / \omega$ . We thus obtain:

$$\bar{P} = g_1 \left( (M_1 E_{2A} - M_2 E_{2B} - M_3 H_B)^2 + (M_2 E_{2A} + M_1 E_{2B} + M_3 H_A)^2 + M_4^2 H_B^2 + M_4^2 H_A^2 \right) / 2 \quad (29)$$

The energy flux inside the ellipsoid is  $\overline{S}_1 = \overline{E}_t \times \overline{H}$ , where  $\overline{E}_t$  and  $\overline{H}$  are given by equations (24) and (20) respectively. We thus obtain:

$$\begin{aligned} \overline{S}_1 = & \left( (M_1 E_{2A} - M_2 E_{2B} - M_3 H_B) H_A \cos^2 \omega t \right. \\ & \left. + (M_2 E_{2A} + M_1 E_{2B} + M_3 H_A) H_B \sin^2 \omega t \right. \\ & \left. + ((M_1 E_{2A} - M_2 E_{2B} - M_3 H_B) H_B + (M_2 E_{2A} + M_1 E_{2B} + M_3 H_A) H_A) \sin \omega t \cos \omega t \right) \hat{k} \\ & + \left( M_4 H_A H_B (\sin^2 \omega t - \cos^2 \omega t) + M_4 \sin \omega t \cos \omega t (H_A^2 - H_B^2) \right) \hat{i} \quad (30) \end{aligned}$$

The time averaged energy flux is  $S_{av} = \int_0^T \overline{S}_1 dt / T$ . We thus obtain:

$$\overline{S}_{av} = \left( (M_1 E_{2A} - M_2 E_{2B}) H_A + (M_2 E_{2A} + M_1 E_{2B}) H_B \right) / 2 (\hat{k}) \quad (31)$$

The induced field makes no contribution to the average energy flux but may contribute significantly to the maximum flux.

Figure 3 illustrates the application of the model to a person near the three-phase transmission line assumed to be located above a perfectly conducting ground (23). The electric field, magnetic field, and energy flux at a distance  $y$  from such a line have been previously computed utilizing an image array induced in the ground (23). Because a human being is small in comparison to the height of the line, the variation of the fields over his or her height is negligible. The person may therefore be modelled as the top half of an ellipsoid which has its image in the ground. A similar technique has been successfully used for the modelling of a rat lying on a conducting plate as the top half of a prolate spheroid (25). We have chosen the dimensions of the ellipsoid to represent an adult human being with a height of 2 m, a trunk breadth of 0.4 m, and a trunk thickness of 0.2 m. Although the direct electric field is independent of the orientation of the ellipsoid about a vertical

axis, the induced field depends on the cross sectional area of the ellipsoid in the X-Z plane, and hence on the orientation of the ellipsoid about a vertical axis. Calculations of the maximum field, power dissipated, and energy flux have been carried out with the greater horizontal axis (0.2 m) in the Z direction. This alignment corresponds to a person facing the transmission line.

## RESULTS

The free space electric and magnetic field components computed at a distance  $y$  from the center-line of the transmission line (23) may be used for  $E_{2A}$  and  $E_{2B}$ , and  $H_A$  and  $H_B$  respectively, to find the internal field, current density, energy stored per unit volume, instantaneous and average power dissipated, and instantaneous and average internal energy flux from equations (25)-(31). Since free space is the external medium,  $K_2 = 1$ , and  $g_2 = 0$ .

Figure 4 illustrates the variation of the maximum internal electric field with distance for a wide range of electrical parameters which have been reported to characterize biological tissues (2). The maximum field occurred in each instance beneath the outer phase and ranged from 0.01 to 0.4 v/m depending of the choice of tissue electrical parameters. The corresponding current densities are 0.01 and 0.004 A/m<sup>2</sup> respectively. At the edge of the right-of-way the internal fields ranged from 0.003 to 0.1 v/m; the corresponding current densities are 0.003 and 0.001 A/m<sup>2</sup>.

Figure 5 gives the maximum power dissipated per unit volume as a function of distance. The energy densities stored in the internal electric and magnetic fields are quite small; the maximum values are, respectively,  $4.96 \times 10^{-6}$  and  $4.41 \times 10^{-2}$  ergs/cm<sup>3</sup>.

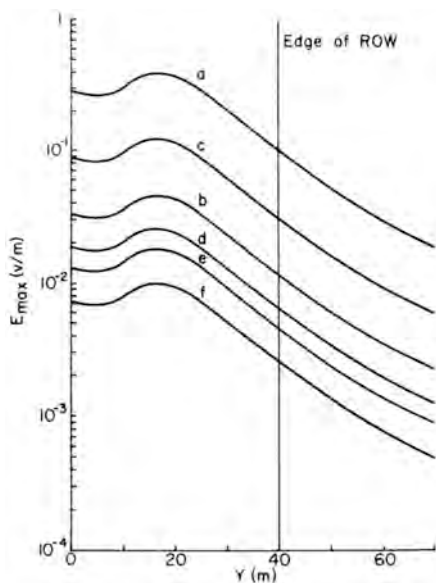


FIGURE 4

Maximum Electric Fields Induced in Ellipsoidal Model of a Human Being Near a 765 KV Transmission Line. Assumed values of dielectric constant and conductivity (mho/m) respectively corresponding to each curve are: (a)  $7 \times 10^5$ , 0.01; (b)  $7 \times 10^5$ , 0.1; (c)  $8 \times 10^6$ , 0.02; (d)  $8 \times 10^6$ , 0.2; (e) 80, 0.33; (f) 80, 1.0. Values apply also to similarly labeled curves in subsequent illustrations.

The maximum and average internal flux levels may be calculated using equations (30) and (31). Although the electric and magnetic fields in free space near the line are essentially in phase, a phase shift may be introduced inside the ellipsoid as represented by  $M_2$  in equation (19). Figures 6 and 7 illustrate the maximum and average energy fluxes inside an ellipsoid at various distances from the line.

## DISCUSSION

As noted above, the induced electric field makes no contribution to the time-averaged energy flux. In addition, the average flux

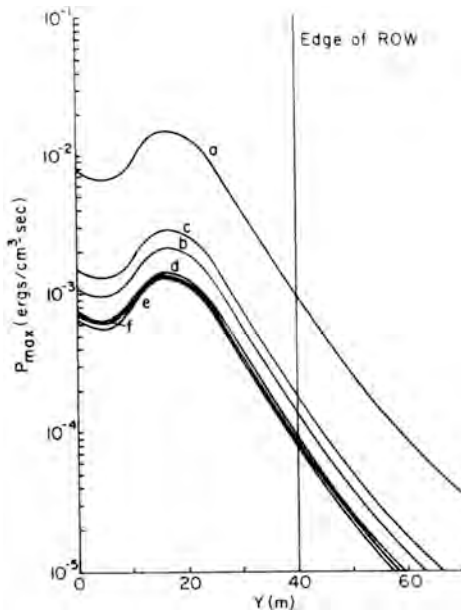


FIGURE 5

Maximum Power Dissipated in an Ellipsoidal Model of a Human Being Near a 765 KV Transmission Line.

displays unusual behavior close to the line, and it may vary widely. When high conductivities and small dielectric constants are assumed, for example, the phase shift of the direct electric field relative to the magnetic field is nearly  $90^\circ$ . The time-averaged flux is thus near zero although peak flux levels are quite high. For these reasons, the maximum energy flux is a more reliable measure of exposure to electromagnetic fields than the average flux if one is considering a wide range of tissue parameters. A similar difference between maximum and average values does not exist for the power dissipated which varies simply as  $E_t^2$ .

It can be seen from Figure 6 that, depending on the tissue constants, the internal ELF flux in an ellipsoidal model of a human

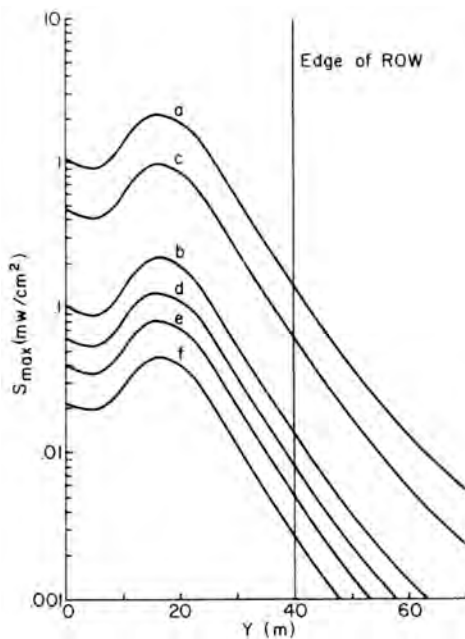


FIGURE 6

Maximum Energy Flux Inside an Ellipsoidal Model of a Human Being Near a 765 KV Transmission Line.

being is as low as the Soviet safety level at 30-60 m from the transmission line. For persons located closer to the line, the internal organs are exposed directly and simultaneously to an energy flux which equals or exceeds the Soviet safety level. At microwave frequencies essentially the only organs which are irradiated directly are the skin, and perhaps the nerves in the dermal net. While the internal ELF fluxes, therefore, are numerically comparable to the Soviet safety level, they differ in that they are simultaneously present at all organs. Thus, extrapolation of microwave exposure levels to lower frequencies may be overly conservative from the viewpoint of the protection provided. The situation is further complicated by the fact that some biological effects due to

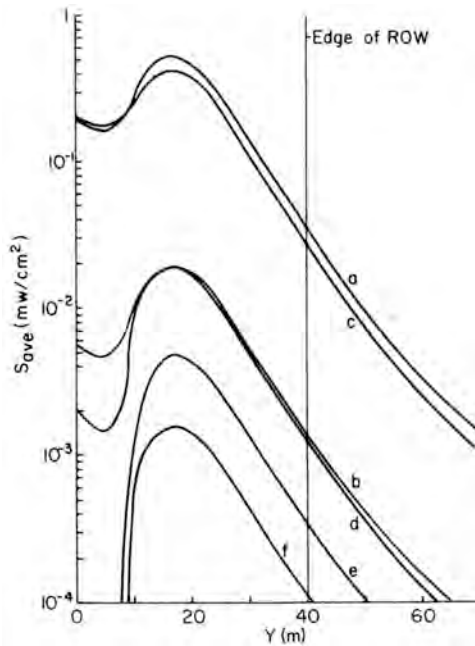


FIGURE 7

Average Energy Flux Inside an Ellipsoidal Model of a Human Being Near a 765 KV Transmission Line.

nonionizing radiation, such as stress, are defined at the whole system level and not at the organ level.

The assumption of perfect ground conductivity leads to higher values of the internal magnetic field, induced electric field, and energy flux. But consideration of the finite-conductivity situation will require detailed specification of the electrical properties of the ground near the array and a considerably more complicated calculation.

The calculations well illustrate the complexities of mathematical modelling of ELF exposure. An ellipsoidal model of a human being is probably the most realistic and accurate morphological choice which allows a solution in closed form. Even so, large variations in the

internal values are found as various characteristics of the ellipsoid are considered.

The variation of the internal electric field, flux, and power density with the shape of the ellipsoid is shown in Table 1. The ellipsoid has  $K_1 = 7 \times 10^5$ , and  $g_1 = 0.1$  mho/m, and is located 40 m from the center-line. All quantities have been evaluated at  $x = 0$ , and  $z = -0.1$ . As the shape is changed from a sphere (row 1) to a prolate spheroid (row 2) to an ellipsoid of increasing eccentricity (rows 3-5), the direct field increases rapidly, but the induced field increases much more slowly. In row 6, as the axis parallel to the magnetic field is changed, the shape again becomes a prolate spheroid. Since the elliptical cross-section normal to  $H$  remains the same as in row 5, the induced field is unchanged while the direct field, which depends on the entire shape, increases significantly. For very eccentric ellipsoids the total field, maximum flux, and power dissipated are determined by the direct field; for relatively symmetrical shapes these quantities are determined by the induced field. The average energy flux, which depends only on the direct field, is particularly sensitive to changes in shape.

A serious difficulty is presented by the lack of acceptable experimental data for the electrical constants of biological tissues (27). Changes in the dielectric constant of the ellipsoid have little effect because at extremely low frequencies  $g_1$  is several times larger than  $\omega K_1 \epsilon_0$  for electrical parameters typical of biological tissue. At audio frequencies such changes would be more significant. The internal electric field, flux, and power dissipated, however, depend strongly on the conductivity of the ellipsoid. This dependence is illustrated in Table 2 for an ellipsoid of  $K_1 = 7 \times 10^5$ ,  $a = 1.67$  m,  $b = 0.4$  m, and  $c = 0.2$  m, located 40 m from the center

TABLE 1  
Variation of Electric Exposure with Shape

a (m)	b (m)	c (m)	$E_{d-max}$ (mV/m)	$E_{i-max}$ (mV/m)	$E_{t-max}$ (mV/m)	$S_{max}$ ( $\mu W/cm^2$ )	$S_{av}$ ( $\mu W/cm^2$ )	$P_{max}$ ( $\mu ergs/cm^3-sec$ )	$P_{max}$ ( $\mu ergs/cm^3-sec$ )
.1	.1	.1	.334	.495	.827	.914	.045	.68	.34
.2	.2	.1	.472	.791	1.26	1.39	.064	1.2	.62
.5	.2	.1	1.31	.951	2.26	2.55	.178	4.2	2.1
1.0	.2	.1	3.43	.979	4.40	5.08	.465	18.0	8.8
2.0	.2	.1	10.0	.987	11.0	12.9	1.36	120.0	58.0
2.0	.1	.1	17.0	.987	18.0	21.2	2.31	320.0	160.0

TABLE 2  
Variation of Exposure with Conductivity

$g$ (mho/m)	$E_{d-max}$ (mV/m)	$E_{i-max}$ (mV/m)	$E_{t-max}$ (mV/m)	$S_{max}$ ( $\mu W/cm^2$ )	$S_{av}$ ( $\mu W/cm^2$ )	$P_{max}$ ( $\mu ergs/cm^3-sec$ )	$P_{max}$ ( $\mu ergs/cm^3-sec$ )
.005	47.8	1.95	49.5	77.9	25.9	120	61
.01	25.7	1.95	27.5	37.8	8.88	76	38
.05	5.27	1.95	7.20	8.40	.842	26	13
.1	2.64	1.95	4.58	5.16	.357	21	10
.5	.527	1.95	2.48	2.66	.06	31	15
1.0	.264	1.95	2.21	2.35	.03	49	24

line. All quantities are evaluated at  $x = 0$ , and  $z = -0.2$  m. The direct field varies approximately inversely with conductivity, unlike the induced field which is independent of the electrical parameters. At low conductivities the total field and maximum energy flux are determined primarily by the direct field, whereas at high conductivities they are determined by the induced field. The averaged energy flux, which depends only on the direct field, decreases rapidly with increasing conductivity. The power dissipated depends on both the conductivity and total field. For small but increasing conductivities, the decrease in the total field causes the power dissipation to also decrease. At high conductivities, however, the total field is primarily determined by the induced field and is nearly independent of conductivity. Consequently, power dissipation passes through a minimum around 0.1 mho/m.

In the ellipsoidal model, the internal values caused by an external ELF flux vary from point to point. The variation of the direct, induced, and total electric fields, the maximum and average fluxes, and the maximum and average power dissipation per unit volume within a cross-section in the X-Z plane is illustrated in Table 3. Values for these quantities at the positions shown in Figure 2 are calculated for an ellipsoid located 40 m from the center-line with  $a = 3.34$  m,  $b = 0.8$  m,  $c = 0.4$  m,  $K_1 = 7 \times 10^5$ , and  $g_1 = 0.1$  mho/m. The direct field is independent of position within the ellipsoid. The magnitude of the induced field for any given  $a'$  and  $c'$  is a maximum for  $|x| = 0$  and decreases as  $|z| \rightarrow 0$ . The total field varies around the ellipse due to the change in both the magnitude and direction of the induced field relative to the direct field. During one half of a cycle, for example, the direct field is pointed downward and the induced field is counter-clockwise. The total field

TABLE 3  
Cross-section Variation of Electrical Exposure

<u>POSITION</u>	<u>x</u> (m)	<u>z</u> (m)	<u>E<sub>d-max</sub></u> (mV/m)	<u>E<sub>i-max</sub></u> (mV/m)	<u>E<sub>t-max</sub></u> (mV/m)	<u>S<sub>max</sub></u> ( $\mu$ W/cm <sup>2</sup> )	<u>S<sub>av</sub></u> ( $\mu$ W/cm <sup>2</sup> )	<u>P<sub>max</sub></u> ( $\mu$ ergs/cm <sup>3</sup> -sec)	<u>P<sub>av</sub></u> ( $\mu$ ergs/cm <sup>3</sup> -sec)
1	0	.2	2.64	1.95	.746	1.14	.357	.56	.28
2	0	-.2	2.64	1.95	4.58	5.16	.357	21	10
3	1.67	0	2.64	.234	2.65	3.13	.357	7.0	3.5
4	-1.67	0	2.64	.234	2.65	3.13	.357	7.0	3.5
5	1.45	.1	2.64	.996	1.69	2.12	.357	2.8	1.4
6	1.45	-.1	2.64	.996	3.61	4.15	.357	13	6.5
7	0	.4	2.64	3.90	1.33	1.75	.357	1.8	.89
8	0	-.4	2.64	3.90	6.52	7.21	.357	43	21
9	0	0	2.64	0	2.64	3.13	.357	6.9	3.5

is then at a minimum at position 1 where the direct and induced fields are opposite in direction, increases through positions 5, 3, and 6, and reaches a maximum at position 2 where the fields have the same direction. The behavior is symmetric for  $x < 0$  as indicated by the identical values at positions 3 and 4. During the other half of the cycle the direction of both the direct and induced field reverses, hence the pattern remains unchanged.

The maximum total field is not exactly equal to the sum of the maxima of the induced and direct fields. The phase shift of the induced field relative to  $H$  is independent of  $K_1$  and  $g_1$ , unlike that of the direct field. The resulting phase difference between the direct and induced fields means that they do not attain their maximum values simultaneously.

The induced field increases with distance from the center, unlike the direct field which is independent of position. The induced field is thus larger at positions 7 and 8 than at 1 or 2, and is in fact larger than the direct field. The total field is then quite large at position 8, but small at position 7.

The average energy flux depends only on the direct field and  $H$ , and thus does not vary over the cross-section. The maximum energy flux displays the same variation with position as the total field, although there may be a phase shift between them. The power dissipated depends only on the total field and thus varies identically with it.

In conclusion, the maximum energy flux and power dissipated are determined primarily by the induced field for relatively symmetrical shapes, high conductivities, and large areas normal to the magnetic field; they are determined primarily by the direct field for

relatively elongated shapes, low conductivities and small areas. In general, both fields will make significant contributions. Because the average energy flux receives no contribution from the induced field and is strongly dependent on the relative phase of the electric and magnetic fields, it is less useful than the maximum flux as a measure of exposure to the electromagnetic field.

#### REFERENCES

- (1) Tolgskaya, M.S. and Gordon, Z.V. *Pathological Effects of Radio Waves*, Consultants Bureau, New York, 1973.
- (2) Presman, A. S. *Electromagnetic Fields and Life*, Plenum Press, New York, 1970.
- (3) Ferri, E.S. and Hagan, G.J. Chronic low-level exposure of rabbits to microwaves. In *Biological Effects of Electromagnetic Waves*, U. S. Department of Health, Education, and Welfare, HEW Publication (FDA) 77-8010, Rockville, Maryland, December 1976, pp. 129-142.
- (4) Mikotajczyk, H. Microwave-induced shifts of gonadotropic activity in anterior pituitary gland of rats. In *Biological Effects of Electromagnetic Waves*, U. S. Department of Health, Education, and Welfare, HEW Publication (FDA) 77-8010, Rockville, Maryland, December 1976, pp. 377-383.
- (5) Sadcikova, M.N. Clinical manifestations of reactions to microwave radiation in various occupational groups. In *Biologic Effects and Health Hazards of Microwave Radiation*. Polls Medical Publishers, Warsaw 1974.
- (6) Novitskiy, Yu I., Gordon, Z.V., Presman, A.S. and Kholodov, Yu A. *RadioFrequencies and Microwaves – Magnetic and Electrical Fields*. Translated from Russian by National Aeronautics and Space Administration, NASA TT F-14, 021, Washington, DC, November 1971.
- (7) Kolodub, F.A. and Yevtushenko, G.I. *Giochemical Aspects of the Biological Effect of a Low-Frequency Pulsed Electromagnetic Field*. U.S. Department of Commerce, NTIS No. JPRS-56583, Springfield, Virginia, July 1972.
- (8) Giarola, A.J. and Krueger, W.F. Continuous exposure of chicks and rats to electromagnetic fields. *IEEE Trans. Microwave Theory Tech.*, vol. **MTT-22**, pp. 432-437, April 1974.

- (9) Cymborowski, B. Influence of electromagnetic field on circadian rhythm of locomotor activity in crickets. *Bulletin De L'Academie Polonaise des Sciences, Serie des Sciences Biologiques*, vol. 3, pp. 713-716, December 1975.
- (10) Becker, R.O. and Marino, A.A. *Electromagnetism and Life*. SUNY Press, Albany, NY 1982.
- (11) Lott, J.R. and McCain, H. Some effects of continuous and pulsating electric fields on brain wave activity on rats. *Int. J. Biometeor.* **17**: 221-225, 1973.
- (12) Batkin, S. and Tabrah, F.L. Effects of alternating magnetic field (12 gauss) on transplanted neuroblastoma. *Research Communications in Chemical Pathology and Pharmacology*, **16**: 351-362, February 1977.
- (13) Friedman, H. and Carey, R.J. Biomagnetic stressor effects in primates. *Physiology and Behavior*, **9**: 171-173, 1972.
- (14) Marino, A.A., Berger, T.J., Austi, B.P., Becker, R.O. and Hart, F.X. In vivo bioelectrochemical changes associated with exposure to extremely low frequency electric fields. *Physiol. Chem. Phys.*, **9**: 433, 1977.
- (15) Noval, J.J., Sohler, A., Reisberg, R.B., Coyne, H., Straub, K.D. and McKinney, H. Extremely low frequency electric field induced changes in rate of growth and brain and liver enzymes of rats. In *Compilation of Navy Sponsored ELF Biomedical and Ecological Research Reports*, Vol 3, U.S. Department of Commerce, NTIS No. AD-A035959, Springfield, Virginia, November 1976.
- (16) Merkulova, L.M. *Histochemistry of Serotonin of Skeletal Muscles Exposed to Pulsed Magnetic Fields*. U.S. Department of Commerce, NTIS No. JPRS-65859, Springfield, Virginia, October 1975.
- (17) Hansson, H. Lamellar bodies in Purkinje nerve cells experimentally induced by electric field. *Brain Research* **216**: 187, 1981
- (18) Marino, A.A., Cullen, J.M., Reichmanis, M., Becker, R.O. and Hart, F.X. Sensitivity to change in electrical environment: a new bioelectric effect. *Am. J. Physiol.* **239**: R424, 1980.
- (19) Perry, F.S., Reichmanis, M., Marino, A.A. and Becker, R.O. Environmental Power-frequency magnetic fields and suicide. *Health Physics* **41**: 267, 1981.
- (20) Bassett, C.A.L., Pilla, A.A. and Pawluk, R.J. A non-operative salvage of surgically-resistant pseudarthroses and non-unions by pulsing electromagnetic fields. *Clin. Orthop.* **124**: 128-143, 1977.

- (21) Wever, R. ELF effects on human circadian rhythms. In *ELF and VLF Electromagnetic Field Effects*. M.A. Persinger, Ed., Plenum Press, New York, 1974, pp. 101-144.
- (22) Hamer, J.R. Effects of low level, low frequency electric fields on human reaction time. *Commun. Behav. Biol.* **2**: 217-222, 1968.
- (23) Hart, F.X. and Marino, A.A. Energy flux along high voltage transmission lines. *IEEE Trans. Biomed. Eng.*, **BME-24**, pp. 493-495, September 1977.
- (24) Schwan, H. P. *Biological Hazards from Exposure to ELF Electrical Fields and Potentials*. Naval Weapons Laboratory, NWL Technical Report TR-2713, Dahlgren, Virginia, March 1972.
- (25) Barnes, H.C., McElroy, A.J. and Charkow, J.H. Rational analysis of live line working. *IEEE Trans. Power App. and Sys.*, vol. **PAS-86**, pp. 482-492, April 1967.
- (26) Spiegel, R.J. High-voltage electric field coupling to humans using method techniques. *IEEE Trans. Biomed. Eng.*, Vol. **BME-24**, pp. 461-472, September 1977.
- (27) Hart, F.X. and Marino, A.A. Biophysics of animal response to an electrostatic field. *J. Biol. Phys.* **4**: 124-143, 1976.
- (28) Stratton, J.A. *Electromagnetic Theory*, McGraw Hill, New York, 1941.
- (29) Seshadri, S.R. *Fundamentals of Transmission Lines and Electromagnetic Fields*. Addison-Wesley, Reading, 1971.
- (30) Magnusson, P.C. *Transmission Lines and Wave Propagation*, Allyn and Bacon, Boston, 1965.
- (31) Sunde, E.D. *Earth Conduction Effects in Transmission Systems*. Dover, New York, 1968.
- (32) Landau, L.D. and Lifshitz, E.M. *Electrodynamics of Continuous Media*. Addison-Wesley, Reading, 1960.